Advanced Composite Materials
Publication details, including instructions for authors and subscription information:
http://www.tandfonline.com/loi/tacm20

Anisomorphic constant fatigue life diagrams for quasi-isotropic woven fabric carbon/epoxy laminates under different hygro-thermal environments

M. Kawai [a] , Y. Yagihashi [a] , H. Hoshi [b] & Y. Iwahori [b]

[a] Department of Engineering Mechanics and Energy , University of Tsukuba , Tsukuba , Ibaraki , 305-8573 , Japan

[b] Advanced Composite Group, Japan Aerospace Exploration Agency , Mitaka, Tokyo , 181-0015 , Japan

Published online: 18 Mar 2013.

To cite this article: M. Kawai , Y. Yagihashi , H. Hoshi & Y. Iwahori (2013) Anisomorphic constant fatigue life diagrams for quasi-isotropic woven fabric carbon/epoxy laminates under different hygro-thermal environments, Advanced Composite Materials, 22:2, 79-98, DOI: 10.1080/09243046.2013.777172

To link to this article: http://dx.doi.org/10.1080/09243046.2013.777172

Advanced Composite Materials, 2013
Vol. 22, No. 2, 79–98, http://dx.doi.org/10.1080/09243046.2013.777172

Anisomorphic constant fatigue life diagrams for quasi-isotropic woven fabric carbon/epoxy laminates under different hygro-thermal environments

M. Kawai[a]*, Y. Yagihashi[a], H. Hoshi[b] and Y. Iwahori[b]

[a]*Department of Engineering Mechanics and Energy, University of Tsukuba, Tsukuba, Ibaraki 305-8573, Japan;* [b]*Advanced Composite Group, Japan Aerospace Exploration Agency, Mitaka, Tokyo 181-0015, Japan*

(*Received 16 March 2012; accepted 6 August 2012*)

The effect of absorbed moisture on the fatigue strength of a plain-weave roving fabric carbon/epoxy quasi-isotropic laminate under constant amplitude loading at different stress ratios has been examined. First, constant amplitude fatigue tests are performed at room and high temperatures (HT), respectively, on the specimens immersed in hot water until saturation as well as on the specimens kept in a dry place. The results indicate that the fatigue lives of wet specimens are shorter than those of dry specimens, regardless of stress ratio as well as test temperature. The fatigue strength is reduced by about 11% due to water absorption at room temperature (RT), regardless of stress ratio. A similar reduction in fatigue strength can be seen in wet specimens at HT as well. Then, the full shapes of constant fatigue life (CFL) diagrams for the woven carbon fiber-reinforced plastic (CFRP) laminate in dry and wet environments are identified using fatigue test data obtained at different stress ratios and at different test temperatures. The results show that the experimental CFL diagrams are asymmetric and nonlinear, and the shape of CFL envelope gradually changes. Finally, the CFL diagrams for the woven CFRP laminate under uniaxial fatigue loading in different hygro-thermal environments are predicted using the anisomorphic CFL diagram approach for composites that was developed in an earlier study. Comparison with experimental results demonstrates that the anisomorphic CFL diagram approach is a promising step in predicting the CFL diagram for the woven CFRP laminate not only in a dry environment but also in a wet environment, regardless of test temperature.

Keywords: CFRP; woven fabric; fatigue; moisture; temperature; S–N relationship; constant fatigue life diagram

1. Introduction

Key application areas that benefit from the high specific stiffness and strength of carbon fiber-reinforced plastics (CFRPs) are rapidly growing, not only in the aerospace sector but also in wind energy,[1] offshore [2] and high performance vehicle [3] sectors. A larger-sized wind turbine is required to enhance efficiency. The diameter of a wind turbine rotor that allows generating more than 5 MW of power, for example, exceeds the length of 100 m.[1] As the length of wind turbine blades increases, a lighter and stiffer material is needed. In deepwater offshore applications, a target water depth of oil and gas drilling is increasing to

*Corresponding author. Email: mkawai@kz.tsukuba.ac.jp

exceed 3,000 m.[4] When they are made of steel, the riser pipes for the target deep sea may suffer from their increased weight and decreased axial rigidity. Such a large riser pipe for deepwater exploration thus requires selecting a material with low weight and high stiffness, in line with a large wind turbine blade. A strong demand for reducing the emissions of carbon dioxide pushes automotive industries to replace conventional materials with composites and to redesign vehicles accordingly.[3]

For reliable application of CFRPs to the components of structures in those key application areas, it is a prerequisite to establish a method for accurately evaluating their fatigue lives under cyclic loading. In other words, it is essential to evaluate the maximum stress levels below which the fatigue lives of their components under constant amplitude cyclic stressing become longer than a specified number of cycles. This is because a fatigue limit that is identified with a stress level below which fatigue life becomes infinite in a given environment cannot clearly be identified in the S–N curves for most continuous carbon fiber composite laminates, unlike most metallic materials. The fatigue analysis of composite structures is thus based on the premise that the fatigue life of a composite for a given loading condition can accurately be predicted.

Fatigue load that composite structures are required to withstand during service differs depending on application. It is characterized by variable amplitude, mean, frequency, and waveform in general. All these factors have significant influences on the fatigue life of composites. Thus, careful consideration of these factors is the key to accurate evaluation of the fatigue lives of composites and composite structures. In this study, we will focus on the effect of the mean stress of a sinusoidal stress–time pattern of constant amplitude and fixed frequency on the fatigue life of CFRP laminates.[5–13]

The effect of mean stress on the fatigue strength of a given composite laminate can conveniently be described using a constant fatigue life (CFL) diagram. In a CFL diagram, alternating stress amplitude is usually plotted against mean stress for different numbers of cycles to failure. The CFL diagrams suitable for CFRPs, unlike metallic materials, were not available until quite recently. Harris et al. [5–11] have quantified the mean stress dependence of fatigue life for various kinds of CFRP laminates, and showed that the CFL envelopes for those composites are nonlinear in shape and asymmetric about the alternating stress axis, and the peak positions are slightly offset to the right of the alternating stress axis. The experimental results obtained from their extensive research work, along with the fatigue data from the other sources,[14–17] suggest that the maxima of CFL envelopes of CFRP laminates correspond to fatigue loading at a stress ratio almost equal to the ratio of compressive strength to tensile strength.

These experimental observations suggest that the linear Goodman diagram,[18] which has successfully been employed in the fatigue analysis of metals, is not always valid for CFRP laminates. It is thus required to establish an engineering method that is suitable for constructing a CFL diagram for CFRP laminates. Adam et al. [7] assumed similar curves for different constant values of fatigue life and proposed an asymmetric parabolic representation of CFL diagram for a composite. Harris et al. [6] found a more general representation of CFL diagram by means of a bell-shape function. Recently, Kawai et al. [16,17] have proposed a different method for efficiently constructing an asymmetric and nonlinear CFL diagram for a given composite on the basis of the static strengths in tension and compression and the reference S–N relationship for a particular stress ratio equal to the ratio of compressive strength to tensile strength. This method was called anisomorphic CFL diagram approach, and shown to be valid for different types of CFRP laminates at room temperature (RT) in a dry environment.[16,17] Accurately constructing the CFL diagrams for composites allows accurately predicting their fatigue lives under constant amplitude fatigue loading at any stress ratios, and

thus efficiently preparing inputs to the fatigue analysis of composites subjected to spectrum loading. The vital importance of the CFL diagrams for composites has more extensively been discussed in Harris [5] and Vassilopoulos [19].

Accurate evaluation of the fatigue lives of CFRP structures also needs consideration of the effects of temperature and moisture, since hygro-thermal environments are often unfavorable for the properties of polymer matrices, especially epoxy resins, in CFRPs.[20,21] The static and fatigue strengths of CFRP at HT are usually lower than those at RT; this tendency has been reported for unidirectional carbon/epoxy laminates [22,23] and for woven fabric carbon/epoxy laminates.[24] A similar reduction in static and fatigue strengths due to temperature has also been observed for carbon fiber-reinforced thermoplastic matrix composites.[25] Regarding the effect of moisture mainly absorbed by the polymer matrices in composites, many experimental studies have revealed that it reduces the tensile strengths of unidirectional carbon/epoxy laminates not only in the transverse direction [26] but also in the fiber direction.[26,27] The reduction in tensile strength due to moisture has also been observed for multidirectional carbon/epoxy laminates of different lay-ups.[28] Ray [29] showed that the interlaminar shear strength of a carbon/epoxy laminate is lowered by water absorption. Patel and Case [30] examined the effect of water absorption on the fatigue damage and strength of woven fabric carbon/epoxy laminates, and found that fiber/matrix decohesion and interlaminar delamination develop more markedly in the specimens that absorbed water, and accordingly the resistance to fatigue is degraded.

These experimental results prove that the fatigue failure of a given CFRP laminate in a wet environment differs from that in a dry environment. It is thus required to establish an engineering method for accurately evaluating the fatigue lives of composites under a variety of hygro-thermal loading conditions that are characterized by a combination of loading waveform, absorbed water content and temperature. If the anisomorphic CFL diagram approach that was developed to predict the fatigue lives of composites for different mechanical loading conditions can be used to predict the fatigue lives of composites exposed to hygro-thermal environments as well, it becomes a more useful and powerful tool for engineering fatigue life analysis of composites.

In the present study, we test the anisomorphic CFL diagram approach for the prediction of fatigue life of composites for its applicability, respectively, to fatigue of a different kind of CFRP laminate (i.e. a woven fabric carbon/epoxy laminate) in dry and wet environments, and to fatigue at different test temperatures. For this purpose, the effects of water absorption on the fatigue lives of the woven CFRP laminate at different stress ratios and at different test temperatures are first discussed. A limited number of constant amplitude fatigue tests at different stress ratios are performed at RT and HT, respectively, on the specimens that were immersed in hot water until saturation as well as on the specimens that were not exposed to water environment but kept in a dry place. By comparing the S–N relationships for the dry and wet specimens that are obtained from testing at different temperatures, the effects of water uptake and temperature on the fatigue lives of the woven CFRP laminate under constant amplitude loading at different stress ratios are observed. The effect of these factors on the shapes of the CFL diagrams in dry and wet environments is also examined. Finally, the S–N relationships for different stress ratios at different temperatures in dry and wet environments are predicted using the anisomorphic CFL diagram approach, and the predictions are compared with experimental results to assess its predictive capability. Because of time-consuming preparation of wet specimens, the number of fatigue data was limited and thus their statistical distribution has not been identified. In this study, therefore, we will confine our attention to observation of the overall effect of water absorption on the fatigue behavior of the woven fabric CFRP laminate at RT and HT and of the potential applicability

of the anisomorphic CFL diagram approach for fatigue life prediction of the woven CFRP laminate in different hygro-thermal environments.

2. Material and testing procedure

2.1. Material and specimen

The material used in this study was a plain-weave roving fabric carbon/epoxy laminate. The woven fabric composite was supplied by TORAY in the form of prepreg sheets (QFC133-6E01A). Twelve-ply quasi-isotropic laminates were fabricated from the prepreg tapes with the stacking sequence of $[(\pm 45)/(0/90)]_{3S}$. The woven carbon/epoxy laminates were cured in an autoclave at 350°F (177 °C). The nominal thickness of as-received laminates was about 2.4 mm.

Two kinds of coupon specimens with different nominal dimensions were prepared. For static tension tests and tension–tension (T–T) fatigue tests, long specimens based on the testing standards JIS K7073 [31] and JIS K7083 [32] were employed; as shown in Figure 1(a), the dimensions of the tensile specimens were gage length $L_G = 100$ mm and width $W = 20$ mm. For static compression tests and compression–compression (C–C) and tension–compression (T–C) fatigue tests, on the other hand, short specimens were used to reduce the risk of buckling of specimens due to compressive load; as shown in Fig. 1(b), the dimensions of the compressive specimens were gage length $L_G = 10$ mm and width $W = 10$ mm. The nominal dimensions of short specimens were determined on the basis of the testing standards JIS K7076 [33] and the report of Harberle and Matthews [34] that discussed suitable methods for compression testing of composite laminates.

A set of tensile and compressive specimens were immersed in hot water of 71 ± 1 °C until saturation, and they are referred to as wet specimens. A water bath with a digital temperature control capability and an automatic water-supply function was used for preparing wet specimens. Another set of tensile and compressive specimens was kept in a dry place at RT, and they are called dry specimens.

On both ends of dry specimens, rectangular-shaped aluminum alloy tabs were glued with epoxy adhesive (Araldite) in order to protect their gripped portions. The thickness of the end-tabs was 1.0 mm for tensile specimens and 2.0 mm for compressive specimens. To wet specimens, however, end-tabs were not attached to avoid drying during their cure process.

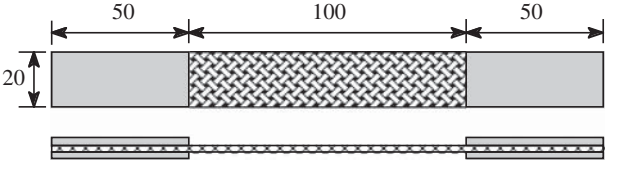

(a) Gauge length 100 mm (tensile specimen)

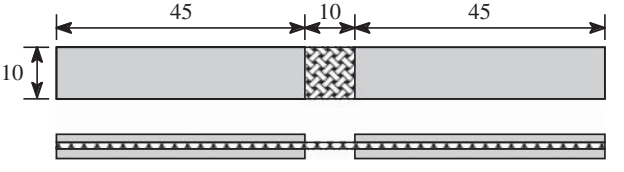

(b) Gauge length 10 mm (compressive specimen)

Figure 1. Specimen geometry (dimension in mm).

Since the 0° layers of the laminate used in this study are protected by the ±45° layers on the surfaces, it is not much hazardous to grip the ends of wet specimens directly.

2.2. Testing procedure

Constant amplitude fatigue tests were carried out on dry and wet specimens under load control at RT (RT ~ 23 °C) and at HT (HT = 80 °C). Fatigue load was applied to specimens in a sinusoidal waveform with a constant frequency of 10 Hz; the fatigue loading condition is based on the testing standard JIS K7083.[32]

Fatigue tests were performed at three different values of stress ratio $R = 0.1$, 10, and χ, where $\chi = \sigma_C/\sigma_T$ and it designates the critical stress ratio that is equal to the ratio of compressive strength σ_C (<0) to tensile strength σ_T (>0).[16,17] Most specimens were fatigue-tested for up to 10^6 cycles. Prior to fatigue testing, static tension and compression tests were performed on dry and wet specimens at RT and HT to identify the tensile and compressive strengths of the woven CFRP laminate in the test environments. The static tests were carried out at a constant rate of 1.0%/min until ultimate failure occurred, following the testing standards JIS K7073.[31] Wet specimens were vaselined except for the gripped portions and then wrapped in a cling film in order to prevent them from drying during fatigue test. It was confirmed that no change occurs in the weight of wet specimens treated as such over the range of time observed up to 4,900 h at RT.

Static and fatigue tests were conducted in 100 kN servo hydraulic MTS-810 machine. For raising the temperature of a specimen, a heating chamber with a precise digital control capability was employed. Each specimen was clamped in the heating chamber by the HT hydraulic wedge grips fitted on the testing machine, and it was heated up to a test temperature in air without applying load and preconditioned in a test environment for 1 h prior to testing. Variation of specimen temperature in time from the prescribed value was less than 1.0 °C. Humidity in the heating chamber was not controlled. The longitudinal and lateral strains of dry specimens in static tests were monitored with two-element L-type rosette strain gages; the gage length of rosettes was 2.0 mm for tension tests and 1.0 mm for compression tests. The strain gages were mounted back to back at the center of each specimen.

3. Experimental results and discussion

The number of experimental data is limited, especially for specimens preconditioned in a wet environment. In this study, therefore, only the qualitative features of the experimental results are observed.

3.1. Water absorption behavior

The moisture absorption behavior of the woven CFRP laminate is first observed. A set of tensile and compressive specimens was immersed in hot water of 71 °C, and the weight of the specimens was measured periodically. The immersion of the specimens in hot water was continued until near saturation of water absorption. The weight gain M_t in percent was calculated using the following equation:

$$M_t = \frac{W_t - W_0}{W_0} \times 100 \tag{1}$$

where W_0 is the initial weight of a dry specimen, and W_t is the current weight of the specimen after t hours of immersion.

Figure 2 shows the relationships between the weight gain and the square root of immersion time for long and short specimens of the woven CFRP laminate. The solid and dashed lines indicate the absorption curves that were obtained by fitting the following simplified equation [35,36] of the solution of the Fick equation [35] to the experimental data:

$$\frac{M_t}{M_\infty} = \tanh\left(\frac{4}{h}\sqrt{\frac{Dt}{\pi}}\right) \tag{2}$$

where M_∞ is the weight gain at saturation, D is the diffusion coefficient, and h is the thickness of specimens. The value of the diffusion coefficient was $2.0 \times 10^{-7}\,\mathrm{mm^2/s}$ for the long specimen and $2.5 \times 10^{-7}\,\mathrm{mm^2/s}$ for the short specimen. The values of diffusion coefficient that were obtained in this study are close to the value of $1.9 \times 10^{-7}\,\mathrm{mm^2/s}$ for the IM7/8551-7 carbon/epoxy laminate.[37] In Figure 2, it is seen that the water absorption process of the woven carbon/epoxy laminate is well described by the Fickian diffusion model. The approximate saturation value of water absorption was about $M_\infty \approx 1.0\%$, and it took 2,500 h (104 days) to reach the approximate saturation level.

3.2. *Static strength*

Comparison of the tensile strengths for dry and wet specimens at RT and HT is shown in Figure 3(a). Similar comparison of the compressive strengths is also presented in Figure 3(b). These figures show the average values of two or three samples. The number of samples is limited, but the possible range of scatter of the static strengths in tension and compression is small. This feature allows us to qualitatively discuss the effects of temperature and moisture on the static and fatigue strengths of the woven CFRP laminate on the basis of a limited number of data.

3.2.1. *Effect of temperature*

The tensile strengths at RT and HT are compared. The ratio of the tensile strength at HT to that at RT was $\sigma_{UTS}^{dry}(\mathrm{HT})/\sigma_{UTS}^{dry}(\mathrm{RT}) = 0.99$ for dry specimens and $\sigma_{UTS}^{wet}(\mathrm{HT})/\sigma_{UTS}^{wet}(\mathrm{RT}) = 0.95$ for wet specimens. These comparisons suggest that while it has no influence of temperature on the tensile strength of a dry specimen, the increase in temperature has a slightly unfavorable influence on the tensile strength of a wet specimen. A similar comparison of compressive

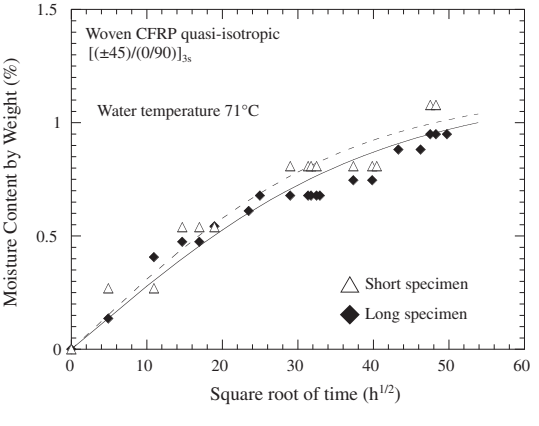

Figure 2. Water absorption curve.

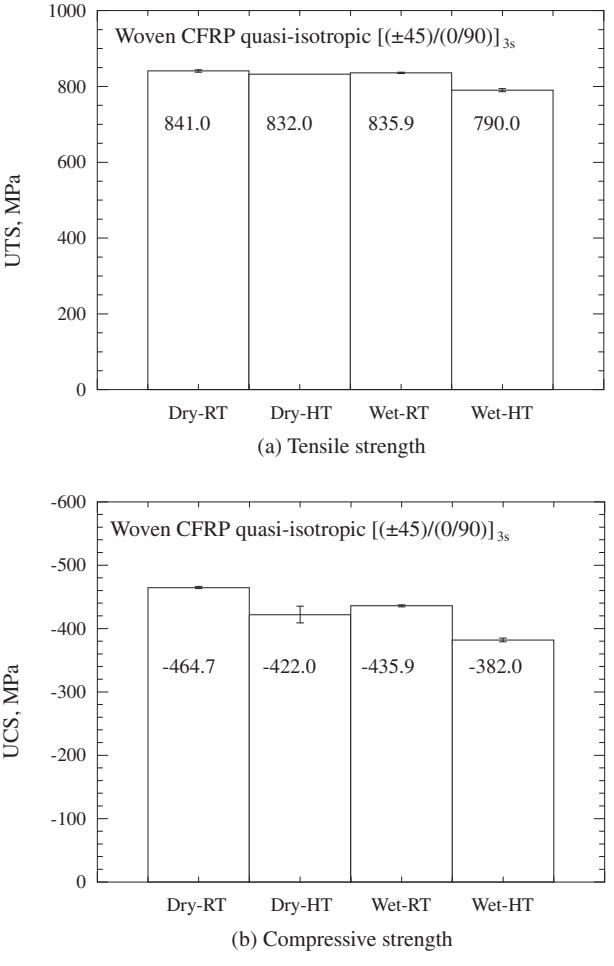

Figure 3. Comparison of static strengths under different hygro-thermal conditions.

strengths led to $\sigma^{dry}_{UCS}(\mathrm{HT})/\sigma^{dry}_{UCS}(\mathrm{RT}) = 0.91$ for dry specimens and $\sigma^{wet}_{UCS}(\mathrm{HT})/\sigma^{wet}_{UCS}(\mathrm{RT}) = 0.88$ for wet specimens. The latter observation reveals that the compressive strength of the woven carbon/epoxy laminate tends to be more significantly reduced by the increase in temperature, regardless of moisture content. The ratio of tensile strength to compressive strength, which gives the critical stress ratio, was $|\chi^{dry}| = |\sigma^{dry}_{UCS}|/\sigma^{dry}_{UTS} = 0.55(\mathrm{RT})$ and 0.51 (HT) for dry specimens, and $|\chi^{wet}| = |\sigma^{wet}_{UCS}|/\sigma^{wet}_{UTS} = 0.52(\mathrm{RT})$ and 0.48(HT) for wet specimens. Obviously, the compressive strength of the woven carbon/epoxy laminate is lower than the tensile strength, regardless of temperature and water absorption.

3.2.2. *Effect of water absorption*

The strengths of dry and wet specimens that were obtained from static tests at the same test temperature are compared to extract the effect of water absorption. The ratio of the compressive strength of wet specimens to that of dry specimens was $\sigma^{wet}_{UCS}(\mathrm{RT})/\sigma^{dry}_{UCS}(\mathrm{RT}) = 0.94$ at RT and $\sigma^{wet}_{UCS}(\mathrm{HT})/\sigma^{dry}_{UCS}(\mathrm{HT}) = 0.91$ at HT. Namely, the compressive strength of wet

specimens at RT was about 6% smaller than that of dry specimens, and the compressive strength of wet specimens at HT was about 9% smaller than that of dry specimens. Thus, the water absorption is apt to moderately reduce the compressive strength of the woven carbon/epoxy laminate, regardless of test temperature.

The effect of water absorption on the tensile strength at RT is considered to be negligible since $\sigma_{UTS}^{wet}(\mathrm{RT})/\sigma_{UTS}^{dry}(\mathrm{RT}) = 0.99$. In contrast, the ratio at HT became $\sigma_{UTS}^{wet}(\mathrm{HT})/\sigma_{UTS}^{dry}(\mathrm{HT}) = 0.95$, thus suggesting that the tensile strength at HT is apt to be reduced by water absorption. A similar tendency of the reduction in tensile and compressive strengths of composites due to water absorption has been reported in literature.[27,29,35] Incidentally, it is considered that the reduction in static strength due to water absorption is caused by the reduction in interlaminar adhesion strength as well as the reduction in the strength of matrix according to the increase in ductility due to water absorption.[38]

3.3. *Fatigue strength*

The S–N relationships at RT are shown in Figures 4 and 5 for dry and wet specimens, respectively. Each figure includes fatigue data for different stress ratios $R = 0.1$, 10, and χ, where $\chi = -0.55$ for dry specimens and $\chi = -0.52$ for wet specimens. The maximum fatigue stress $\sigma_{\max}$ is plotted against the logarithm of the number of reversals to failure $2N_f$ in the case $R = 0.1$ and χ, while the absolute value of minimum fatigue stress $|\sigma_{\min}|$ is plotted in the case $R = 10$. From these figures, it can clearly be observed that the S–N relationship for the woven carbon/epoxy laminate significantly depends on the shape of load waveform (i.e. the value of stress ratio in the present context), regardless of the degree of water absorption.

It has been reported that the gradient of S–N relationship becomes largest under fatigue loading at the critical stress ratio.[16,17] Observing the results in Figure 4 for dry specimens and Figure 5 for wet specimens, we can confirm that it is also true for the woven carbon/epoxy laminate tested in this study, and the gradient of S–N relationship becomes largest under fatigue loading at the critical stress ratio, regardless of moisture content.

Comparisons of the S–N relationships for dry and wet specimens are shown in Figure 6 (a)–(c) for different stress ratios $R = 0.1$, 10, and χ, respectively. We can clearly observe that the fatigue lives of wet specimens are shorter than those of dry specimens, regardless of stress ratio. While the number of fatigue data is limited, the fatigue strength of wet specimens can be estimated to be about 11% lower than that of dry specimens, regardless of stress ratio.

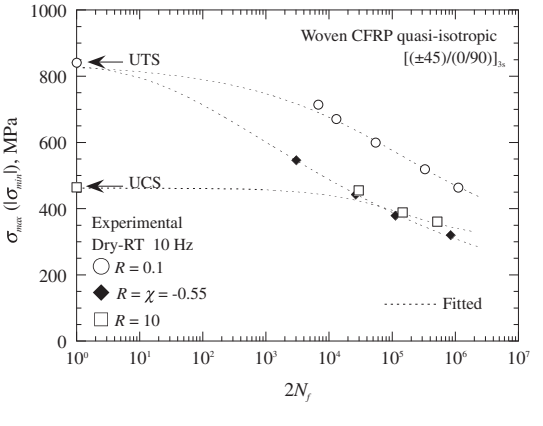

Figure 4. S–N relationships for dry specimens at RT.

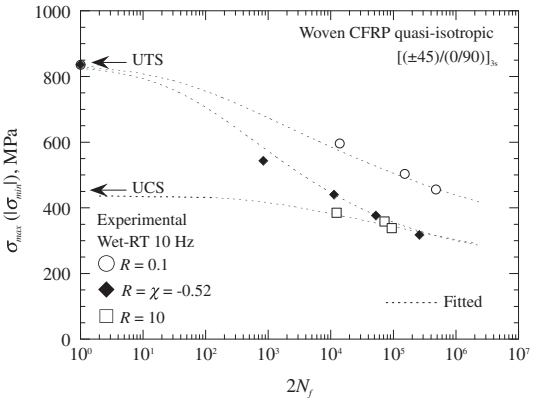

Figure 5. S–N relationships for wet specimens at RT.

The reduction in fatigue strength is affected by the reduction in static strength in general. As observed above, $\sigma_{UTS}^{wet}(\mathrm{RT})/\sigma_{UTS}^{dry}(\mathrm{RT}) = 0.99$, and thus the difference between the tensile strengths of dry and wet specimens at RT is negligible. This fact reveals that lower fatigue strengths of wet specimens for $R = 0.1$ and χ that can be seen in Figure 6(a) and (b) were caused by the absorption of water.

On the other hand, the above observation that $\sigma_{UCS}^{wet}(\mathrm{RT})/\sigma_{UCS}^{dry}(\mathrm{RT}) = 0.94$ suggests that the compressive strength of the woven carbon/epoxy laminate was reduced by water absorption. Therefore, it is considered that the difference between the S–N relationships for the dry and wet specimens fatigue loaded at $R = 10$ that was observed in Figure 6(c) is affected by the reduction in compressive strength due to water absorption. To observe the effect of moisture on the fatigue strength of the woven carbon/epoxy laminate for $R = 10$, the fatigue data for dry and wet specimens were normalized with respect to their compressive strengths. Figure 7 shows the normalized S–N relationships for the dry and wet specimens that were fatigue loaded at $R = 10$. There is a tendency for the relative fatigue resistance to be slightly reduced by water absorption under C–C fatigue loading at $R = 10$, which is consistent with the above observations for $R = 0.1$ and χ at RT. On the fatigue strength at HT, a similar degrading effect of water absorption was observed. For reference, the fatigue data obtained at HT are presented in Figures 8 and 9, and Figure 10(a)–(c) in the same manner as in the results at RT.

3.4. Experimental CFL diagram

The effect of moisture absorption on the CFL diagram for the woven carbon/epoxy laminate is examined. The experimental CFL diagram can be constructed by plotting alternating stress against mean stress. Figures 11 and 12 show the experimental CFL diagrams for dry and wet specimens at RT, respectively. In these figures, the experimental data points for different constant values of life were evaluated using the S–N curves fitted to the experimental S–N data; they are indicated by dashed lines in Figures 4–10. The dashed lines in Figures 11 and 12 indicate the CFL envelopes for different values of life that were predicted using the anisomorphic CFL diagram approach.[16,17]

While more fatigue data for different stress ratios are necessary to identify the shape of CFL diagram, the plots of CFL data in Figures 11 and 12 strongly suggest that the overall shape of the CFL diagram for the woven carbon/epoxy laminate at RT becomes asymmetric

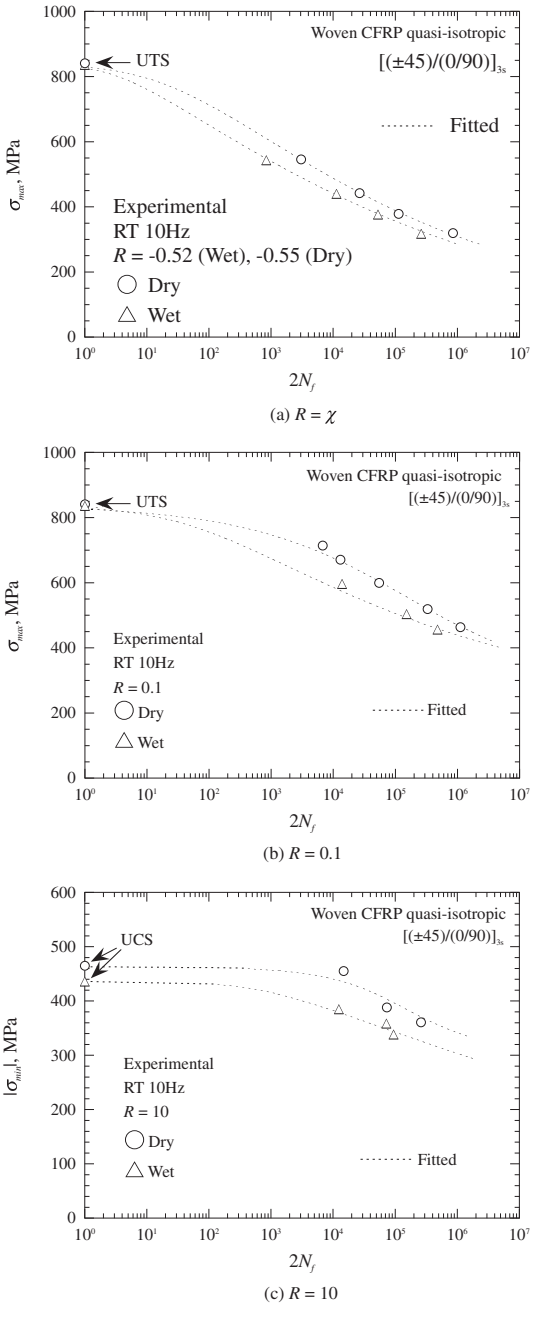

Figure 6. Comparison of S–N relationships for dry and wet specimens at RT.

about the alternating stress axis, and the shape of CFL envelope changes as the number of cycles to failure increases. As guided by the dashed lines, the CFL envelope is almost linear in the range of a short life, but it turns nonlinear in the range of a longer life. The peak of the CFL envelope is slightly offset to the right of the alternating stress axis, and it is

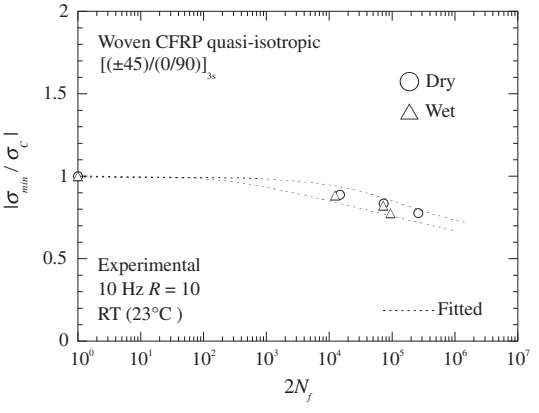

Figure 7. Normalized S–N relationships for dry and wet specimens at RT.

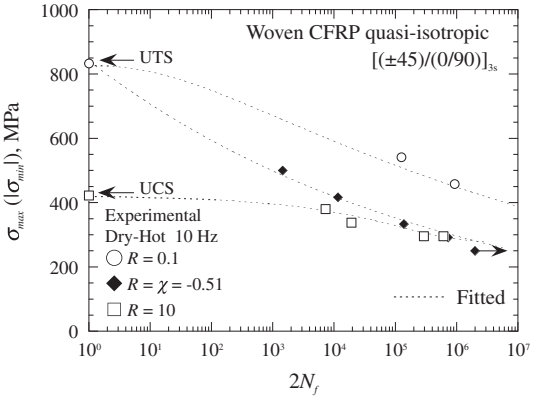

Figure 8. S–N relationships for dry specimens at HT.

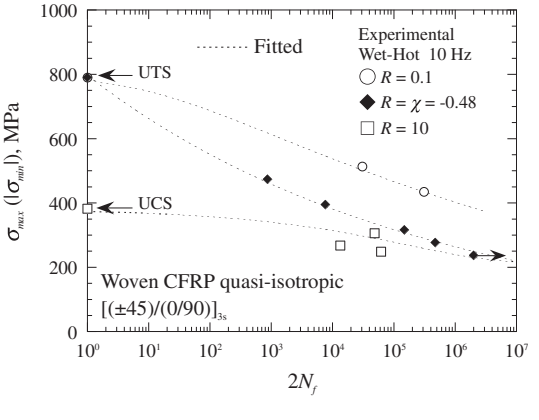

Figure 9. S–N relationships for wet specimens at HT.

associated with the stress ratio close to the ratio of compressive strength to tensile strength, i.e. $\chi = -0.55$. This means that the maximum alternating stress is accompanied not by T–C fatigue loading at $R = -1$ but by T–C fatigue loading at the critical stress ratio $R = \chi$.

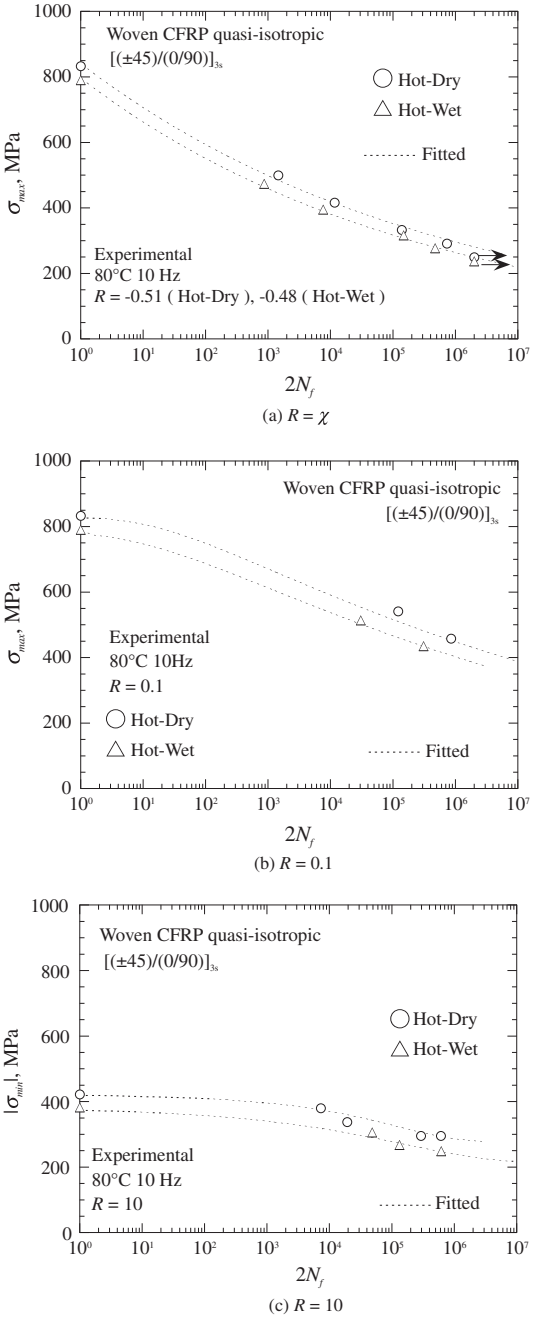

Figure 10. Comparison of S–N relationships for dry and wet specimens at HT.

The shape of the CFL diagram for wet specimens is similar to that for dry specimens, as can be seen in Figure 12. The difference between the CFL diagrams for dry and wet specimens is small, since the difference between the absolute values of tensile and compressive

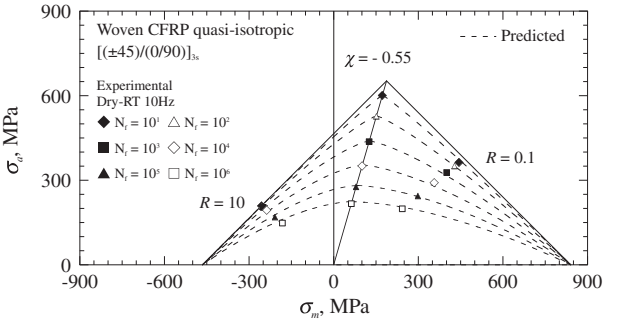

Figure 11. Anisomorphic CFL diagram for dry specimen at RT.

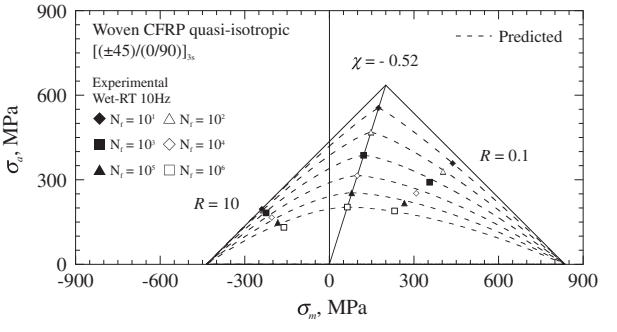

Figure 12. Anisomorphic CFL diagram for wet specimen at RT.

strengths for these specimens is small and the critical stress ratio for wet specimens $\chi = -0.52$ is close to that for dry specimens $\chi = -0.55$, accordingly.

Consequently, the experimental results suggest the following features: (1) the CFL diagram for the woven carbon/epoxy laminate is asymmetric about the alternating stress axis, (2) the shape of CFL envelope changes in shape from a straight line to a nonlinear curve as the number of cycles to failure increases, (3) the peaks of CFL envelopes correspond to fatigue loading at the critical stress ratio, and (4) these features are common to the CFL diagrams for dry and wet environments.

4. Theoretical CFL diagram

If the CFL diagram for a composite that is exposed to a hygro-thermal environment is identified over the whole range of mean stress $\sigma_C \leqslant \sigma_m \leqslant \sigma_T$, one can efficiently predict the fatigue life of the composite for any constant amplitude fatigue loading in the given hygro-thermal environment. Therefore, it is a practical demand to establish such a CFL diagram approach in the form that is suitable for composites. The experimental results obtained from this study, along with the results from other sources,[6–11,14–17] suggest not only that the symmetric and linear Goodman diagram is not always valid for CFRP laminates, but also that a CFL diagram constructed using the equi-life envelopes of similar shape for different constant values of life cannot be justified for all kinds of composite laminates.

The anisomorphic CFL diagram that was recently proposed by Kawai et al. [16,17] takes account of all the fundamental requirements that are suggested by the experimental results

reported so far. The anisomorphic CFL diagram was shown to be valid for different types of non-woven CFRP laminates in a dry environment at RT. A generalization attempt has also been made to enhance the flexibility of the anisomorphic CFL diagram approach by which it can be applied to the fatigue behavior of composites that exhibit more complicated sensitivity to mean stress in fatigue loading.[39]

If the anisomorphic CFL diagram is applicable to woven carbon/epoxy laminates not only in a dry environment but also in different hygro-thermal environments, the potential usefulness of this approach for evaluating the fatigue life of composites can be justified further. In order to answer this question, therefore, the anisomorphic CFL diagram approach is further tested on the woven carbon/epoxy laminates that are exposed to different hygro-thermal environments.

4.1. *Anisomorphic CFL diagram*

The anisomorphic CFL diagram [16,17] is a theoretical CFL diagram that can be constructed for a given composite using only the static strengths in tension and compression and a single reference S–N relationship for the critical stress ratio χ. It allows predicting the S–N curves for the composite for any stress ratios in a given environment.

A brief review of this method is presented for the sake of convenience. The CFL envelope for a given constant value of life is composed of two smooth members that are defined in the two intervals of mean stress and associated with tension and compression dominated failure modes, respectively. The two member curves are connected with each other on the radial straight line with a particular constant value of amplitude ratio $\sigma_a/\sigma_m = \sigma_a^{(\chi)}/\sigma_m^{(\chi)} = (1-\chi)/(1+\chi)$ that is associated with the critical stress ratio χ. The theoretical CFL curves are described by means of a piecewise nonlinear function that is defined by different formulas depending on the position of mean stress σ_m in the interval $[\sigma_C, \sigma_T]$ as follows:

$$-\frac{\sigma_a - \sigma_a^{(\chi)}}{\sigma_a^{(\chi)}} = \begin{cases} \left(\frac{\sigma_m - \sigma_m^{(\chi)}}{\sigma_T - \sigma_m^{(\chi)}}\right)^{2-\psi_\chi}, & \sigma_m^{(\chi)} \leqslant \sigma_m \leqslant \sigma_T \\ \left(\frac{\sigma_m - \sigma_m^{(\chi)}}{\sigma_C - \sigma_m^{(\chi)}}\right)^{2-\psi_\chi}, & \sigma_C \leqslant \sigma_m < \sigma_m^{(\chi)} \end{cases} \tag{3}$$

where σ_C (<0) and σ_T (>0) are the compressive and tensile strengths of the composite considered, respectively. The key quantities $\sigma_a^{(\chi)}$ and $\sigma_m^{(\chi)}$ represent the alternating and mean stress components, respectively, of the maximum fatigue stress $\sigma_{\max}^{(\chi)}$ for a given constant value of life N_f under T–C fatigue loading at the critical stress ratio $\chi = \sigma_C/\sigma_T$;

$$\sigma_a^{(\chi)} = \frac{1}{2}(1-\chi)\sigma_{\max}^{(\chi)} \tag{4}$$

$$\sigma_m^{(\chi)} = \frac{1}{2}(1+\chi)\sigma_{\max}^{(\chi)} \tag{5}$$

The variable ψ_χ in Equation (3) denotes the fatigue strength ratio for loading at the critical stress ratio χ, and it is defined as

$$\psi_\chi = \frac{\sigma_{\max}^{(\chi)}}{\sigma_T} \tag{6}$$

Accordingly, $0 \leqslant \psi_\chi \leqslant 1$. Note that the tendency to tensile fatigue failure is equivalent to the tendency to compressive fatigue failure, i.e. $\sigma_{\max}/\sigma_T = \sigma_{\min}/\sigma_C$, only under T–C fatigue loading at the critical stress ratio χ that is not always equal to –1 in the case of fiber-reinforced composites, since they are asymmetric in tension and compression in general.

The reference S–N curve for the critical stress ratio is described in a normalized form by means of a continuous monotonic function of the number of cycles to failure $2N_f = f(\psi_\chi)$. It is useful to assume a particular form of the function that is given by

$$2N_f = \frac{1}{K_\chi}\frac{1}{(\psi_\chi)^n}\frac{\langle 1-\psi_\chi\rangle^a}{\langle \psi_\chi - \psi_{\chi(L)}\rangle^b} \tag{7}$$

where the angular brackets $\langle\rangle$ denote the singular function defined as $\langle x\rangle = \max\{0,\ x\}, \psi_{\chi(L)}$ is a normalized fatigue limit. The coefficients K_χ, n, a, b, and $\psi_{\chi(L)}$ designate material constants, and they are determined by fitting Equation (7) to the reference fatigue data for the critical stress ratio.

If the exponent $M = 2 - \psi_\chi$ in the piecewise-defined function is replaced with a constant value of unity, the anisomorphic CFL diagram can be reduced to the following form [40]:

$$-\frac{\sigma_a - \sigma_a^{(\chi)}}{\sigma_a^{(\chi)}} = \begin{cases} \frac{\sigma_m - \sigma_m^{(\chi)}}{\sigma_T - \sigma_m^{(\chi)}}, & \sigma_m^{(\chi)} \leqslant \sigma_m \leqslant \sigma_T \\ \frac{\sigma_m - \sigma_m^{(\chi)}}{\sigma_C - \sigma_m^{(\chi)}}, & \sigma_C \leqslant \sigma_m < \sigma_m^{(\chi)} \end{cases} \tag{8}$$

which represents the asymmetric Goodman diagram. If ψ_χ is eliminated from the exponent, the formulas for the anisomorphic CFL diagram become

$$-\frac{\sigma_a - \sigma_a^{(\chi)}}{\sigma_a^{(\chi)}} = \begin{cases} \left(\frac{\sigma_m - \sigma_m^{(\chi)}}{\sigma_T - \sigma_m^{(\chi)}}\right)^2, & \sigma_m^{(\chi)} \leqslant \sigma_m \leqslant \sigma_T \\ \left(\frac{\sigma_m - \sigma_m^{(\chi)}}{\sigma_C - \sigma_m^{(\chi)}}\right)^2, & \sigma_C \leqslant \sigma_m < \sigma_m^{(\chi)} \end{cases} \tag{9}$$

which is equivalent to the asymmetric Gerber diagram.[38] A more systematic review of advanced modeling of CFL diagram for uniaxial fatigue loading of composites has been presented in [41].

4.2. Comparison with experimental results

The dashed lines in Figures 11 and 12 indicate the anisomorphic CFL diagrams predicted. The solid line in each figure by which the anisomorphic CFL diagram is bounded corresponds to static failure $\psi_\chi = 1$. In these figures, it is seen that for both dry and wet specimens, the experimental CFL data for $R = 0.1$ and 10 are in good agreements with the predicted CFL envelopes, regardless of temperature and moisture content. Note that the fatigue data for $R = 0.1$ and 10 were not used for predicting the anisomorphic CFL diagrams for dry and wet specimens. The fatigue data used in constructing the anisomorphic CFL diagram are those for only the critical stress ratio. Thus, we can use the fatigue data for $R = 0.1$ and 10 to verify the anisomorphic CFL diagram approach. Consequently, the good agreements between predictions and observations for these stress ratios suggest that the anisomorphic CFL diagram approach has great potential as a preliminary tool for visualizing the mean stress dependence of fatigue life of the woven carbon/epoxy laminate in different hygro-thermal environments.

Using these anisomorphic CFL diagrams, we can predict S–N relationships for constant amplitude fatigue loading at any stress ratios for different temperature and moisture environments. The predicted S–N curves for dry and wet specimens at RT are shown in Figures 13 and 14, respectively, along with the corresponding experimental data. It is clearly seen that the predicted S–N curves for $R = 0.1$ and 10 agree well with the experimental results, regardless of moisture content, which is consistent with the good agreements between the predicted and experimental CFL diagrams. These comparisons thus prove that the anisomorphic CFL diagram approach has the potential of giving reasonable predictions of the fatigue lives of the woven carbon/epoxy laminate in a wet environment as well as in a dry environment.

Similar comparisons of predictions for dry and wet environments at 80 °C are shown in Figures 15–18. In Figures 15 and 16, it is seen that the observed asymmetric and nonlinear CFL diagrams in dry and wet environments at 80 °C agree well with those predicted using the anisomorphic CFL diagram approach. Accordingly, the S–N relationships for different stress ratios that were predicted using the anisomorphic CFL diagrams correlate well with the experimental S–N data, as seen in Figures 17 and 18. Inspecting these predictions in a more detail, however, we notice that optimistic predictions were made for $R = 10$ at 80 °C. In order to evaluate the accuracy of prediction using the present method, more data would be required especially for $R = 10$, since the S–N relationship for C–C loading at $R = 10$ has a small

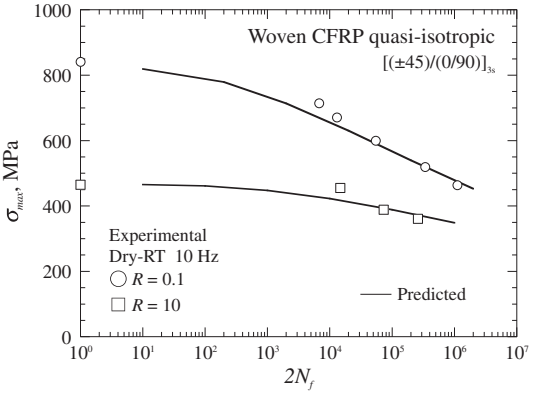

Figure 13. Predicted S–N relationships for dry specimens at RT.

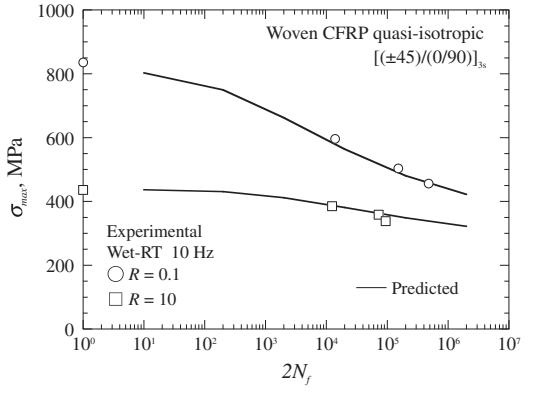

Figure 14. Predicted S–N relationships for wet specimens at RT.

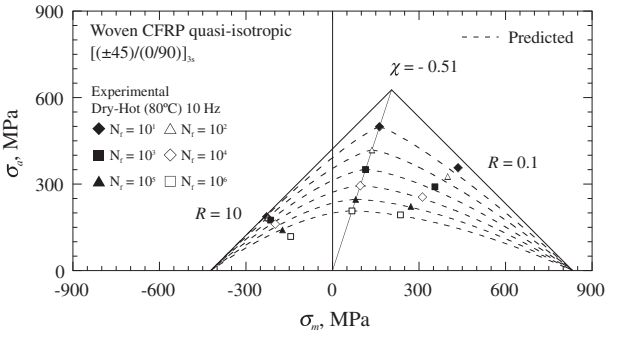

Figure 15. Anisomorphic CFL diagram for dry specimen at HT.

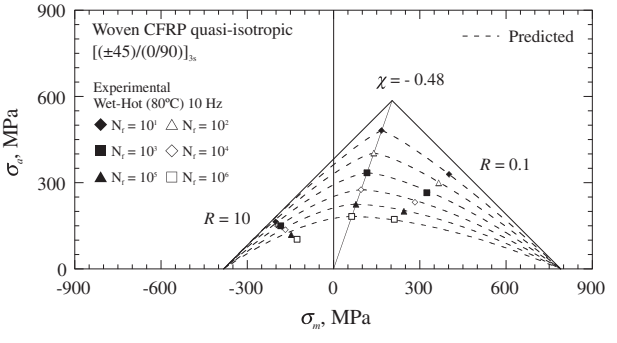

Figure 16. Anisomorphic CFL diagram for wet specimen at HT.

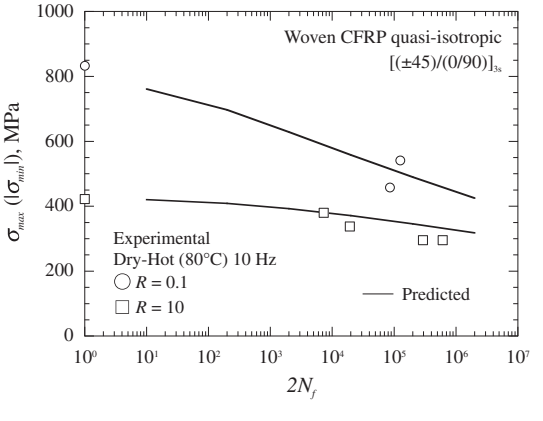

Figure 17. Predicted S–N relationships for dry specimens at HT.

gradient, and it is apt to be unfavorably affected by the scatter of data particularly in such a case. While it involves the limitation of the number of fatigue data especially for wet environments, the present study has succeeded in suggesting a potential usefulness of the anisomorphic CFL diagram approach for prediction of fatigue life of the woven carbon/epoxy laminate in different hygro-thermal environments.

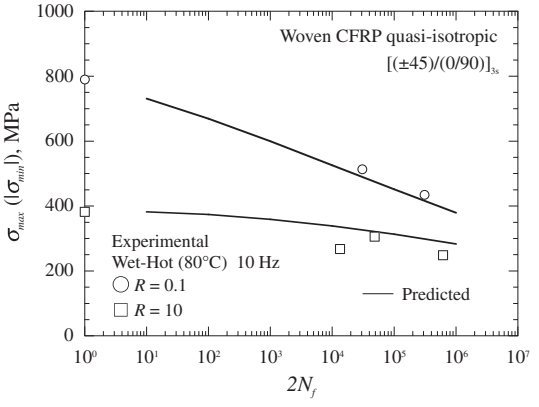

Figure 18. Predicted S–N relationships for wet specimens at HT.

5. Conclusions

The anisomorphic CFL diagram approach was tested on plain-weave roving fabric carbon/epoxy quasi-isotropic laminates that were exposed to different hygro-thermal environments. For this purpose, a limited number of constant amplitude fatigue tests were performed on the woven carbon/epoxy laminates in dry and wet environments at different stress ratios and at different temperatures. The effect of a combination of water absorption and temperature on the fatigue strength of the woven carbon/epoxy laminate was distilled from these experimental results. They were used to assess the overall applicability of the anisomorphic CFL diagram approach. The results obtained can be summarized as follows:

(1) The fatigue lives of wet specimens tend to become shorter than those of dry specimens at RT, regardless of stress ratio. The reduction in fatigue strength due to water absorption was about 11%.
(2) A similar reduction in fatigue strength due to water absorption occurred at HT (80 °C).
(3) Stress ratio has a significant influence on the S–N relationship for the woven carbon/epoxy laminate, regardless of temperature and moisture content.
(4) The slope of S–N relationship became largest for fatigue loading at the critical stress ratio, regardless of temperature and moisture content.
(5) The experimental CFL diagram for the woven carbon/epoxy laminate exhibits asymmetry and nonlinearity, regardless of test temperature and moisture content. The peaks of CFL envelopes are accompanied by fatigue loading at the critical stress ratio. The difference between the critical stress ratios for dry and wet specimens is small because of small difference between the static strengths in tension and compression. Accordingly, no significant difference in shape was observed between the CFL diagrams for dry and wet specimens.
(6) The anisomorphic CFL diagrams predicted for different moisture–temperature conditions agree well with the CFL diagrams suggested by a limited amount of experimental data. Accordingly, the S–N curves for the woven carbon/epoxy laminate that were predicted using the anisomorphic CFL diagram are in good correlation with the experiment S–N curves, regardless of water content, temperature, and stress ratio. The good agreements between the predicted and observed results suggest that the anisomorphic CFL diagram approach is a promising step in predicting fatigue lives of

the woven carbon/epoxy laminate at different temperatures not only in a dry environment but also in a wet environment.

Acknowledgment

This study was supported in part by the Ministry of Education, Culture, Sports, Science and Technology of Japan under a Grant-in-Aid for Scientific Research (No. 20360050).

References

[1] Kensche C. Fatigue of composites for wind turbines. Int. J. Fatigue 2006;28:1363–1374.
[2] Gustafson C, Echtermeyer A. Long-term properties of carbon fibre composite tethers. Int. J. Fatigue 2006;28:1353–1362.
[3] Feraboli P, Masini A. Development of carbon/epoxy structural components for a high performance vehicle. Composites: Part B. 2004;35:323–330.
[4] Watanabe Y, Ito N, Suzuki H, Tamura K. Optimization of a multiple traplock structure of CFRP riser pipe for deep sea drilling. In: Proceedings of the 17th International Offshore and Polar Engineering Conference. 2007 Jul 8; Lisbon. p. 864–870.
[5] Harris B, editor. Fatigue in composites. Cambridge: Woodhead Publishing Limited; 2003.
[6] Harris B, Reiter H, Adam T, Dickson RF, Fernando G. Fatigue behaviour of carbon fibre reinforced plastics. Composites 1990;21:232–242.
[7] Adam T, Fernando G, Dickson RF, Reiter H, Harris B. Fatigue life prediction for hybrid composites. Int. J. Fatigue 1989;11:233–237.
[8] Harris B, Gathercole N, Lee JA, Reiter H, Adam T. Life-prediction for constant-stress fatigue in carbon-fibre composites. Phil. Trans. Roy. Soc. Lond. 1997;A355:1259–1294.
[9] Adam T, Gathercole N, Reiter H, Harris B. Fatigue life prediction for carbon fibre composites. Adv. Compos. Lett. 1992;1:23–26.
[10] Gathercole N, Reiter H, Adam T, Harris B, Life prediction for fatigue of T800/5245 carbon-fibre composites: I. Constant-amplitude loading. Fatigue. 1994;16:523–532.
[11] Beheshty MH, Harris B, Adam T. An empirical fatigue-life model for high-performance fibre composites with and without impact damage. Composites: Part A. 1999;30:971–987.
[12] Kawai M. A phenomenological model for off-axis fatigue behavior of unidirectional polymer matrix composites under different stress ratios. Composites: Part A. 2004;35:955–963.
[13] Kawai M, Suda H. Effects of non-negative mean stress on the off-axis fatigue behavior of unidirectional carbon/epoxy composites at room temperature. J. Compos. Mater. 2004;38:833–854.
[14] Ramani SV, Williams DP. Notched and unnotched fatigue behavior of angle-ply graphite/epoxy composites. In: Reifsnider KL, Lauraitis KN, editors. Fatigue of filamentary composite materials. Philadelphia: ASTM STP 636, 1977; Madrid. p. 27–46.
[15] Ansell MP, Bond IP, Bonfield PW. Constant life diagrams for wood composites and polymer matrix composites. In: Proceedings of the Ninth International National Conference on Compos. Mater. (ICCM 9), Vol. V. 1993; Madrid. p. 692–699.
[16] Kawai M. A method for identifying asymmetric dissimilar constant fatigue life diagrams of CFRP laminates. Key Eng. Mater. 2007;334–335:61–64.
[17] Kawai M, Koizumi M. Nonlinear constant fatigue life diagram for carbon/epoxy laminates at room temperature. Composites: Part A. 2007;38:2342–2353.
[18] Goodman J. Mechanics applied to engineering. Harlow: Longman; 1899.
[19] Vassilopoulos AP, editor. Fatigue life prediction of composites and composite structures. Cambridge (UK): Woodhead Publishing Limited; 2010.
[20] Zhou J, Lucas JP. Hygrothermal effects of epoxy resin. Part I: the nature of water in epoxy. Polymer 1999;40:5505–5512.
[21] Zhou J, Lucas JP. Hygrothermal effects of epoxy resin. Part II: variations of glass transition temperature. Polymer 1999;40:5513–5522.
[22] Kawai M, Yajima S, Hachinohe A, Takano Y. Off-axis fatigue behavior of unidirectional carbon fiber-reinforced composites at room and high temperatures. J. Compos. Mater. 2001;35:545–576.
[23] Kawai M, Sagawa T. Temperature dependence of off-axis tensile creep rupture behavior of a unidirectional carbon/epoxy laminate. Composites: Part A. 2008;39:523–539.

[24] Kawai M, Taniguchi T. Off-axis fatigue behavior of plain woven carbon/epoxy composites at room and high temperatures and its phenomenological modeling. Compos. Part A 2006;37:243–256.
[25] Jen MR, Tseng Y, Kung H, Hung JC. Fatigue response of APC-2 composite laminates at elevated temperatures. Composites: Part B. 2008;39:1142–1146.
[26] Kriz RD, Stinchcomb WW. Effects of moisture residual thermal curing stresses, and mechanical load on the damage development in quasi-isotropic laminates. In: Reifsnider KL, editor. Damage in Composite Materials. Philadelphia: ASTM STP 775. 1982; p. 63–80.
[27] Shen C, Springer GS. Effects of moisture and temperature on the tensile strength of composite materials. J. Compos. Mater. 1977;11:2–16.
[28] Garg AC. Effect of moisture and temperature on fracture behavior of graphite–epoxy laminates. Eng. Fract. Mech. 1988;29:127–149.
[29] Ray BC. Temperature effect during humid ageing in interfaces of glass and carbon fibers reinforced epoxy composites. J. Colloid Interf. Sci. 2006;298:111–117.
[30] Patel SR, Case SW. Durability of a graphite/epoxy woven composite under combined hygrothermal conditions. Int. J. Fatigue 2000;22:809–820.
[31] JIS K7073. Testing method for tensile properties of carbon fiber-reinforced plastics. Japanese Industrial Standard, Japanese Standards Association; 1988.
[32] JIS K7083. Testing method for constant-load amplitude tension–tension fatigue of carbon fiber-reinforced plastics. Japanese Industrial Standard, Japanese Standards Association; 1993.
[33] JIS K7076. Testing method for compressive properties of carbon fiber-reinforced plastics. Japanese Industrial Standard, Japanese Standards Association; 1991.
[34] Haberle JG, Matthews FL. An improved technique for compression testing of unidirectional fibre-reinforced plastics; development and results. Composites: Part A. 1994;5:358–371.
[35] Shen CH, Springer GS. Moisture absorption and desorption of composite materials. J. Compos. Mater. 1976;10:2–20.
[36] McKague EL, Jr, Reynolds JD, Halkias JE. Moisture diffusion in fiber reinforced plastics. ASME J. Eng. Mater. Technol. 1976;98:92–95.
[37] Silverman E, Wiacek CR, Griese RA. Characterization of IM7 graphite/thermoplastic polyetheretherketone (PEEK) for spacecraft structural applications. In: Grimes GC editor. Composite Materials: Testing and Design (Tenth Volume). Philadelphia: ASTM STP 1120. 1992; p. 118–130.
[38] Yagihashi Y, Hoshi H, Kawai M, Iwahori Y. Effects of water uptake on fatigue behavior of CFRP quasi-isotropic laminates. In: Proceedings of the JSME Annual Meeting. 2008 Aug 3–7; Yokohama.
[39] Kawai M, Murata T. A three-segment anisomorphic constant life diagram for the fatigue of symmetric angle-ply carbon/epoxy laminates at room temperature. Composites: Part A. 2010;41:1498–1510.
[40] Kawai M, Shiratsuchi T, Yang K. A spectrum fatigue life prediction method based on the nonlinear constant fatigue life diagram for CFRP laminates. In: Proceedings of the Sixth Asia–Australasian Conference Compos. Mater. (ACCM-6). 2008 Sep 23–26; Kumamoto, Kyushu, Japan. p. 153–156.
[41] Kawai M. Fatigue life prediction of composite materials under constant amplitude loading. In: Vassilopoulos AP, editor. Fatigue life prediction of composites and composite structures. Cambridge (UK): Woodhead Publishing Limited; 2010. p. 177–219.